ISSN 0915-633X

NATIONAL INSTITUTE FOR FUSION SCIENCE

Eigenfunction Spectrum Analysis for Self-organization in Dissipative Solitons

N. Kondo and Y. Kondoh

(Received - Oct. 11, 1995)

NIFS-380 Oct. 1995

RESEARCH REPORT
NIFS Series

NAGOYA, JAPAN

Eigenfunction Spectrum Analysis for Self-organization in Dissipative Solitons

Nobukazu Kondo and Yoshiomi Kondoh

Department of Electronic Engineering, Gunma University,

Kiryu, Gunma 376, Japan

abstract

An attractor of dissipative structures in solitons described by the Korteweg-de Vries(KdV) equation with a viscous dissipation term is investigated, with the use of an eigenfunction spectrum analysis associated with the dissipative dynamical operator [Phys. Rev. E **49**(1994)5546]. It is shown numerically and quantitatively that the basic procesess for the self-organization of dissipative soliton are spectrum transfer by nonlinear interaction and selective dissipation among the eigenmodes of the dissipative operator. It is quantitatively shown that an interchange between the dominant operators occurs during nonlinear self-organization processes, which leads to a final self-similar coherent structure uniquely determined by the dissipative operator.

Keywords: self-organization, eigenfunction spectrum analysis, KdV equation, soliton, dissipative operator, spectrum transfer, selective dissipation,

1 Introduction

In non-linear dissipative dynamical systems, ordered structures to each system have attracted much attention in many fields of research. This general concept, referred to as "dissipative structure" or "self-organization" has been introduced in thermodynamic systems by I. Prigogine[1, 2]. It includes force-free fields of cosmic magnetism[3], two-dimensional viscous fluids [4, 5], and solitons described by the Korteweg-de Vries(KdV) equation with frictional dissipation[6, 7]. One of the authors (Y. K.) has recently proposed a theory of general self-organization[8, 9] to find attractors of the dissipative structure. The theory clarifies that the realization of coherent structures in time evolution is equivalent to that of self-organaized states with the minimum change rate of autocorrelation for their instantaneous values. It leades to that the atrractors are given by eigenfunctions for dissipative dynamic operators[8, 9] in dynamic systems of interest.

Generally, dynamical systems of interest having n variables $q_i(t, \mathbf{x})$, with $i = 1, 2, ...n$, may be described by the following equation:

$$\frac{\partial q_i}{\partial t} = L_i^N[\mathbf{q}] \; + \; L_i^D[\mathbf{q}] \, , \tag{1}$$

where $L_i^N[\mathbf{q}]$ and $L_i^D[\mathbf{q}]$ denote respectively the nondissipative and dissipative dynamic operators which may be either linear or nonlinear [8, 9]. When the value of $L_i^N[q]$ is large, then the profile of q is significantly changing in time. When the system comes close to the equilibrium state, i.e., when the value of $L_i^N[q]$ is vary small, then the dominant operator changes from $L_i^N[q]$ to $L_i^D[q]$. The final self-organized profile, which is one from among the set of equilibria satisfying $L_i^N[q] = 0$, will be determined uniquely by the operators $L_i^D[q]$, which are relatively dominant during the later phase of the self-organization process. The dynamic behavior of the self-organization processes and the realization of coherent structures in dissipative dynamical systems will become clear through the use of spectra on the eigenfunctions for the dissipative dynamic operator[12, 13]. Generally, the selective dissipation of the spectrum components of the eigenmodes may be shown through the use of the trigonometric functions(e.g. the Fourier analysis) or other orthogonal functions except eigenfuctions for dissipative dynamic operators. However, the use of these orthogonal functions does not lead to the self-similar change phase of the final self-organized state, if those functions are not the eigenfunction for the dissipative operators.

In this paper, using the eigenfunction spectrum analysis associated with the dissipative operators, we will numerically and quantitatively show that the three basic processes for the self-organization in viscously dissipative solitons are spectrum transfer and selective dissipation among the eigenmodes of the dissipative operators $L_i^D[\mathbf{q}]$, and interchange between the dominant operators from the nondissipative nonlinear operators $L_i^N[\mathbf{q}]$ to the dissipative operators $L_i^D[\mathbf{q}]$ in later phase of self-organization. We will also show that the final coherent structure in viscously dissipative solitons is the lowest eigenmode of the dissipative operator. In Sec.2, we present a basic theory of self-organization for dissipative solutions by KdV equation with a viscous term. Numerical analysis for results of simulation and discussion are presented in Sec.3.

2 Basic Theory of Self-Organization

We investgate the self-organization process for solitons described by the following KdV equation with a viscous dissipation term[14]:

$$\frac{\partial q}{\partial t} + q\frac{\partial q}{\partial x} + \delta^2\frac{\partial^3 q}{\partial x^3} = \eta\frac{\partial^2 q}{\partial x^2} \,. \tag{2}$$

Here δ is a constant, η is the coefficient of viscosity, and the nondissipative and dissipative operators $L_i^N[\mathbf{q}]$ and $L_i^D[\mathbf{q}]$ of Eq.(1) correspond respectively to the $-q\partial q/\partial x - \delta^2\partial^3 q/\partial x^3$ term and the $\eta\partial^2 q/\partial x^2$ term in Eq.(2). In the absence of dissipation ($\eta = 0$), the energy corresponding to the autocorrelation $W_{ii} = \int_0^b q(t,x)\cdot q(t,x)\mathrm{d}x$ is conserved, where b is the periodicity length. The rate of energy dissipation $\partial W_{ii}/\partial t$ due to the viscous term in Eq.(2) is $-2\int_0^b \eta(\partial q/\partial x)^2\mathrm{d}x$. The self-organized state q^* is defined as that state for which the rate of change is minimum for the autocorrelation of instantaneous values [8, 9]. The mathematical expressions for the above definition are written as follows, with the use of a functional F with a Lagrange multiplier α:

$$F \equiv -\frac{\partial W_{ii}}{\partial t} - \alpha W_{ii} \,, \tag{3}$$

$$\delta F = 0 \,, \tag{4}$$

$$\delta^2 F > 0 \,, \tag{5}$$

where $F = \int_0^b[2\eta(\partial q/\partial x)^2 - \alpha q^2]\mathrm{d}x$. Integrating by parts, we obtain

$$\delta F = -2\int_0^b \delta q\Big[\,2\eta\frac{\partial^2 q}{\partial x^2} + \alpha q\,\Big]\mathrm{d}x = 0 \,, \tag{6}$$

$$\delta^2 F = -2\int_0^b \delta q\Big[\,\eta\frac{\partial^2 \delta q}{\partial x^2} + \frac{\alpha}{2}\delta q\,\Big]\mathrm{d}x > 0 \,, \tag{7}$$

where δF and $\delta^2 F$ are the first and second variations of F with respect to the variation δq only for the spatial variable x, and the periodicity constraint has been applied. Then, the Euler-Lagrange equation for an arbitrary variation δq is obtained from Eq.(6), as follows[14]:

$$\frac{\partial^2 q^*}{\partial x^2} + \lambda^2 q^* = 0 . \quad (8)$$

Here the parameter λ is defined by $\lambda^2 \equiv \alpha/2\eta$, and q^* denotes the self-organized state corresponding to minimal rate of change of the autocorrelation. The eigenfunctions of Eq.(8) can be obtained for given boundary values of q as boundary value problems. Using the same procedure in ref. [8, 9], we obtain the following:

$$\frac{\partial W ii^*}{\partial t} = -\alpha\, W_{ii}^* , \quad (9)$$

$$q^* = q_{\mathrm{R}}^* \mathrm{e}^{-(\alpha/2)t} , \quad (10)$$

$$q_{\mathrm{R}}^* = A \sin(\lambda_1 x + \phi) . \quad (11)$$

Here $W_{ii}^* \equiv \int_0^b q^*(t,x) \cdot q^*(t,x) \mathrm{d}x$; q_{R}^* is the solution of Eq.(8) for the self-organized state q^* under the periodicity condition; and the Lagrange multiplier is $\alpha = 2\eta\lambda_1^2$, with λ_1 the smallest positive eigenvalue that yields minimized rate of change for the autocorrelation of instantaneous values[9]. From Eq.(7), we obtain the following associated eigenvalue problems for the critical perturbations δq that make $\delta^2 F$ to vanish[8, 9]:

$$\frac{\partial^2 \delta q_k}{\partial x^2} + \lambda_k^2 \delta q_k = 0. \quad (12)$$

Here $\lambda_k^2 = \alpha_k/2\eta$, λ_k and α_k are the eigenvalues, and δq_k denotes the eigensolutions. In the present periodic boundray condition, the eigensolution of Eq.(8) becomes the eigenfunction with the smallest eigenvalue λ_1 of Eq. (12). The eigenfunctions a_k for associated eigenvalue problem of Eq.(12) form a complete orthogonal set and the appropriate normalization is written as

$$\int a_k \cdot \Big[\frac{\partial^2 a_j}{\partial x^2}\Big] \mathrm{d}V \;=\; \int a_j \cdot \Big[\frac{\partial^2 a_k}{\partial x^2}\Big] \mathrm{d}V \;=\; \lambda_k^2 \int a_j \cdot a_k \mathrm{d}V \;=\; \lambda_k^2 \delta_{jk}, \qquad (13)$$

where $\partial^2 a_k/\partial x^2 + \lambda_k^2 a_k = 0$ is used. For the present case under the periodicity condition, the normalized orthogonal eigensolutions of a_k is obtained as follows:

$$a_k \;=\; \sqrt{\frac{2}{b}} \sin(\lambda_k x \;+\; \phi_k) \;, \qquad (14)$$

where $\lambda_k = 2\pi k/b$, and $k(= 1, 2, 3 \cdots)$ is the mode number.

We consider here the root mean square average of the nondissipative term, N_d , and that of dissipative term, D_d , which are given by $D_d = \frac{1}{b}\sqrt{\int_0^b \Big(\eta \frac{\partial^2 q}{\partial x^2}\Big)^2 \mathrm{d}x}$, $N_d = \frac{1}{b}\sqrt{\int_0^b (q - d_0)^2 \Big(\frac{\partial q}{\partial x}\Big)^2 \mathrm{d}x}$, where d_0 is the constant component of q. In order to investgate the dominantly working operator, we introduce two quantities of D and N, defined respectively by $D = D_d/(D_d + N_d)$ and $N = N_d/(D_d + N_d)$. We call here D and N as "the dissipative ratio" and "the nondissipative ratio", respectively. By substituting Eq.(11) into N_d and D_d, the values of D and N at the self-organized state are obtained as follows:

$$D \;=\; \frac{2\eta\lambda_1}{A + 2\eta\lambda_1} \,, \qquad (15)$$

$$N \;=\; \frac{A}{A + 2\eta\lambda_1} \,. \qquad (16)$$

Since the amplitude A in the later phase of self-organization becomes small, it is seen from Eqs.(15) and (16) that $D \sim 1$ and $N \sim 0$ for $A \ll 2\eta\lambda_1$. Therefore, we recognize that the final self-similar coherent structure is determined uniquly by the dissipative dynamical operator $\eta\partial^2 q/\partial x^2$.

The profile of q distributions at each instant can be expanded by using orthogonal eigenfunctions a_k for the eigenvalue problem of Eq.(12) as follows[8, 9]:

$$q = \sum_{k=1}^{\infty} c_k a_k \,, \tag{17}$$

where c_k is the eigenmode spectrum components. It should be noted here that the spectrum component of c_1 by this eigenfunction expantion corresponds to the basic components q^*, and that the spectra of $c_k(_k= 1, 2, 3, \cdots)$ depend upon time t. From product of the eigenfunction a_k of Eq.(14) and spatiotemporal data of the simulation results, we obtain numerically the components c_k of eigenmode spectrum at each time. When the profile of q at each time is decomposed into the eigenfunction spectrum c_k assocaited with the dissipative dynamical operator, the following three procesess will be shown: (1)The nondissipative nonlinear interaction of the solitons induces the spectrum transfer towards both the higher and lower eigenmode regions. (2)At the same time, since there exists a limit to the lower eigenmode, the spectrum transfer towards the lower eigenmode region may yield spectrum accumulation at the lowest eigenmode[13, 17]. (3)The dissipative operator $\eta\partial^2 q/\partial x^2$ causes the higher energy spectral components to dissipate more rapidly, with decay constants of $\alpha = 2\eta\lambda_k^2$, while the lowest eigenmode λ_1 remains until the end.

3 Results and Discussion

For the numerical simulations, we used a new type of numerical scheme for hyperbolic equations, named the 1D 2nd KOND-H scheme, which has a high numerical accuracy and stability through the use of the Kernel Optimum Nearly-Analytical Discretization(KOND) Algorithm[15, 16]. Double precision is employed for these calculations. Using the same process as shown in Fig. 10 of Ref.[16], we first obtained a numerical solution having four solitons per periodicity length for the KdV equation without the dissipative term, i.e. $\eta = 0$ in Eq.(2). With the use of this multi-soliton solution as the initial profile, the self-organization process of the solitons in the presence of dissipation is investigated. Four typical cases with viscosity $\eta = 0.02$, 0.03, 0.04 and 0.08 were calculated respectively, with the use of the same parameters of $b = 50$, and $\delta = 0.42$.

Figures 1(a)-(d) show the typical time evolution of the self-organization process for dissipative solitons for the case with $\eta = 0.02$, where the vertical scale is varied to accommodate the magnitude of the numerical amplitudes at each time. Figure 1(a) is the initial profile at $t = 0$ of four solitons per periodicity length, where the four solitons are labeled as q_{m1}, q_{m2}, q_{m3} and q_{m4} in order from the largest to the smallest. In Fig.1(b) at $t = 200$, the third soliton q_{m3} is interacting with the first soliton q_{m1}, and energy transfer from the smaller soliton to the larger soliton is occurring. The energy of the fourth soliton has been almost absorbed into the first soliton q_{m1} during the interaction with it in Fig.1(b). In Fig.1(c) at $t = 1000$, after the two smaller solitons q_{m3} and q_{m4} have been absorbed into the larger solitons, the interaction and absorption of the second soliton q_{m2} into the first q_{m1} continues to occur. In Fig.1(d) at $t = 4000$, all three smaller solitons q_{m4}, q_{m3} and q_{m2} have been absorbed into the first one q_{m1}. This implies that the energy of smaller solitons has been transferred finaly into that of the largest soliton during interactions involving viscous dissipation. It is found from Fig.1(d) that the lowest eigensolution of Eq.(11) has become the final self-organized state in this nonlinear dissipative system.

Figures 2(a)-(d) show the typical time evolutions of the energy spectrum components c_k^2 for the case with $\eta = 0.02$, where the spectrums are normalized by the maximum component in each figure, and k is the mode number. The numeral integers in the figures indicate typical mode numbers. Figure 2(a) is the spectrum for the initial profile at $t = 0$. It is recognized from Fig.2(b) at t=200 that the energy spectrum has been transferred simultaneously towards both the higher and lower eigenmode regions from the initially given spectrum, in other words, the normal and inverse energy cascades[10, 11] occur during the nonlinear interactions of dissipative solitons. From Fig.2(c) at t=1000, it is found that the rate of decrease of the higher components are larger than the lower ones. Consequently, we recognize that the selective dissipation occurs among the eigenmodes of the dissipative operators. From Fig.2(d) at t=4000, it is found that the coherent attractor of the lowest eigenmode of $k = 1$ has been realized in the final self-organized state in this non-linear dissipative system.

Figure 3 shows the time dependence of the dissipative ratio D and nondissipative ratio N defined after by Eqs.(15) and (16). Here, (D_2, N_2), (D_3, N_3), (D_4, N_4), and (D_8, N_8) denote respectively the data for the cases with $\eta = 0.02, 0.03, 0.04$ and 0.08 . The values of D and N at the initial profile are $N > D$. The values of D increase, while those of N decrease, and the two lines of D and N cross at the vertical level of 0.5. Since the interchange time of the dominant operator is represented by the intersection of the two lines of D and N, we find from the numerical data used for Fig.3 that the dominant operator changes around at $t = 3500$ for $\eta = 0.02$, $t = 1200$ for $\eta = 0.03$, $t = 800$ for $\eta = 0.04$, and $t = 150$ for $\eta = 0.08$. After the dominant operator changes, the interchange of the two operators is no longer observed until the end of these runs of simulation. These results clearly show that an interchange between the dominant operators has occurred in its approach towards the final self-similar coherent solution of Eq.(11), which is determined uniquely by the dissipative operator $\eta\partial^2 q/\partial x^2$.

Figure 4 shows the time dependence of the energy (on a natural logarithmic scale) defined by $W_{ii} = \frac{1}{b}\int_0^b (q - d_0)^2 dx$. After the period of a rapid decay has passed, each decay rate of the energy is seen to become almost constant. The decay constant has values of 0.665×10^{-3} for $\eta = 0.02$, 0.962×10^{-3} for $\eta = 0.03$, 1.29×10^{-3} for $\eta = 0.04$ and 2.59×10^{-3} for $\eta = 0.08$. On the other hand, since the smallest eigenvalue is $\lambda_1 = 2\pi/50$, the theoretical values of the decay constant α in Eq.(9) are 0.632×10^{-3} for $\eta = 0.02$, 0.943×10^{-3} for $\eta = 0.03$, 1.26×10^{-3} for $\eta = 0.04$ and 2.53×10^{-3} for $\eta = 0.08$. We find that the simulation results agree fairly well with the theoretical values of decay constant $\alpha = 2\eta\lambda_1^2$.

4 Conclusion

We have confirmed numerically and quantitatively the following basic processes for the self-organization in viscously dissipative solitons, using the eigenfunction spectrum analysis associated with the dissipative dynamic operator $\eta\partial^2 q/\partial x^2$. (1) During dissipative nonlinear interactions, the spectrum transfer and selective dissipation among the eigenmodes of the spectrum components occur in the self-organization phenomena of dissipative solitons[cf. Fig.2(b)-(d)]. (2) In the later phase of self-organization, there occurs the interchange between the dominant operators from the nondissipative nonlinear operator to the dissipative operator[cf. Fig.3], which leads to the final coherent structure uniquely determined by the dissipative operator.

5 Acknowledgment

The authors wish to acknowledge valuable discussions with Messers. M. Yamaguchi, and A. Nakano and Dr. J. W. Van Dam at Institute for Fusion Studies, University of Texas at Austin. This work was carried out under the collaborative research program at the Natoinal Institute for Fusion Science, Nagoya, Japan.

References

[1] I. Prigogine, *Etude Thermodynamique des Phenomenes Irreversibles* (Dunod, Paris, 1974).

[2] I. Prigogine and P. Glansdorff, *Thermodynamic Theory of Structure, Stability, and Fluctuations* (Wiley-Interscience, New York, 1971).

[3] S. Chandrasekhar and L. Woltjer, Proc. Natl. Acad. Sci. **44** 285(1958).

[4] R. H. Kraichnan and D. Montgomery: Rep. Prog. Phys. **43** (1980) 35.

[5] M. Hossain, W.H. Matthaeus and D. Montgomery: J. Plasma Phys. **30** (1983) 479.

[6] A. Hasegawa, Y. Kodama and K. Watanabe: Phys. Rev. Let. **47** (1981) 1525.

[7] A. Hasegawa: Adv. Phys. **34** (1985) 1.

[8] Y. Kondoh: Phys. Rev. E **48** (1993)2975.

[9] Y. Kondoh: Phys. Rev. E **49** (1994) 5546.

[10] R. Horiuchi and T. Sato: Phys. Fluids **29** (1986)1161.

[11] R. Horiuchi and T. Sato: Phys. Fluids **31** (1988)1142.

[12] Y. Kondoh, Y. Hosaka, J. Liang, R. Horiuchi and T. Sato: J. Phys. Soc. Jpn. **63** (1994) 546.

[13] Y. Kondoh, T. Yumoto, M. Yamaguchi, N. Kondo, R. Horiuchi, T. Sato: Nucl. Fusion **71** (1995)432.

[14] Y. Kondoh and J. W. Van Dam: Phys. Rev. E **52** (1995)1721.

[15] Y. Kondoh: J. Phys. Soc Jpn. **60** (1991) 2851.

[16] Y. Kondoh, Y. Hosaka and K. Ishii: Computers Math. Applic. **27** (1994) 59.

[17] N. Kondo, Y. Kondoh: "*Eigenfunction Spectrum Analysis for Self-organization Process*", Nucl. Fusion **71** (1995) No9 in press.

Figure captions

Fig. 1. Typical time evolution of solitary wave forms during self-organization in the case of $\eta = 0.02$: (a) initial profile at $t = 0$, with the four solitons denoted as q_{m1}, q_{m2}, q_{m3}, and q_{m4} in order of size; (b) at $t = 200$; (c) at $t = 1000$; (d) at $t = 4000$.

Fig. 2. Typical time evolution of the energy spectrum C_k^2 during self-organization in the case of $\eta = 0.02$: (a) initial profile at $t = 0$, with the mode number of k(1,2, 3, $\cdots$); (b)at $t = 200$; (c) at $t = 1000$; (d) at $t = 4000$.

Fig. 3. Time dependence of the dissipative ratio D and the nondissipative ratio N. (D_2, N_2), (D_3, N_3), (D_4, N_4), and (D_8, N_8) denote respectively the data for the cases with $\eta = 0.02, 0.03, 0.04$ and 0.08 .

Fig. 4. Time dependence of the energy W_{ii} (on a natural logarithmic scale) per perriodicity length.

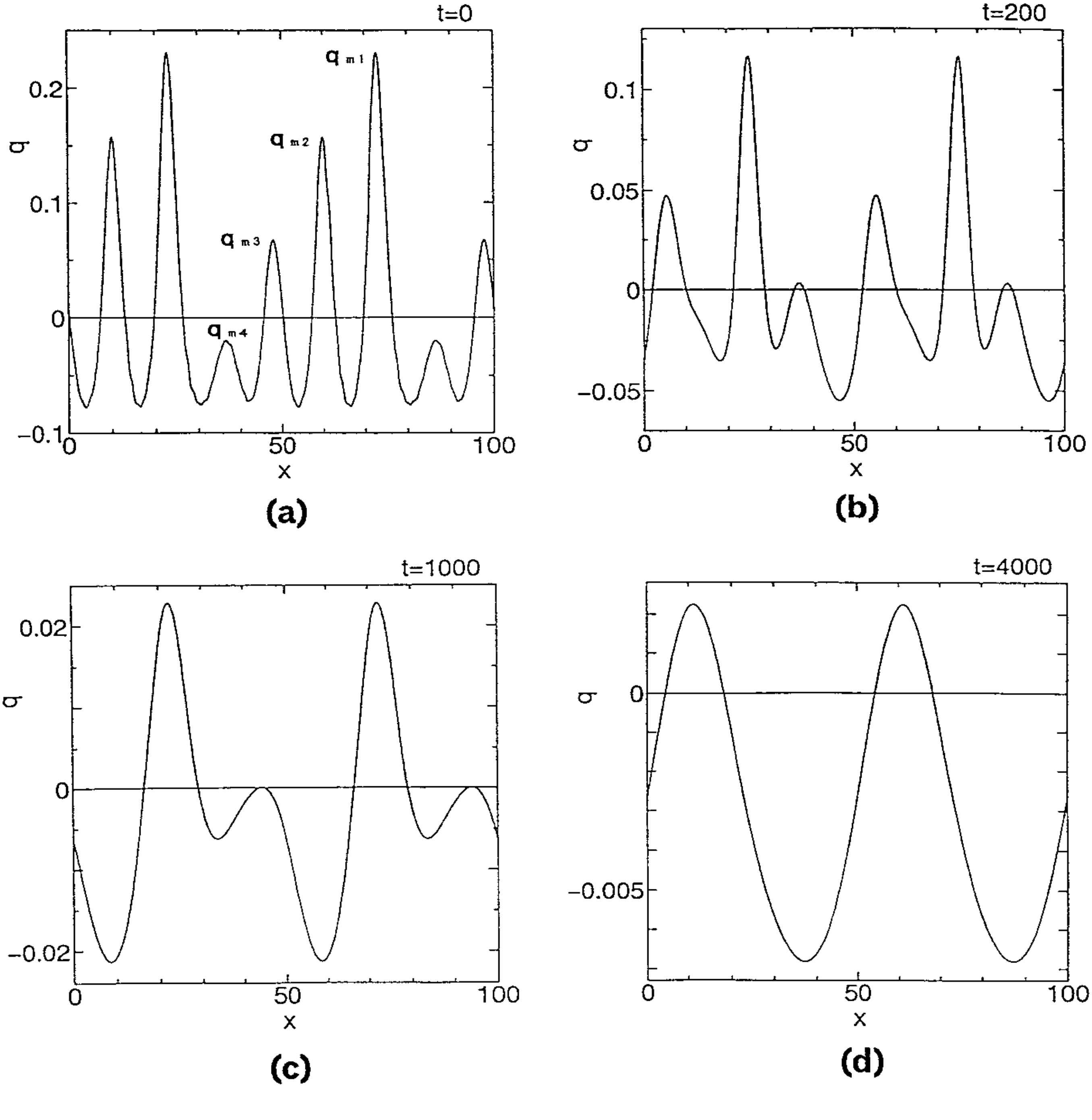
t=0
q
0.2
0.1
0
−0.1
q m1
q m2
q m3
q m4
0
50
100
x
(a)
t=200
0.1
0.05
0
−0.05
(b)
t=1000
0.02
−0.02
(c)
t=4000
−0.005
(d)

Fig. 1

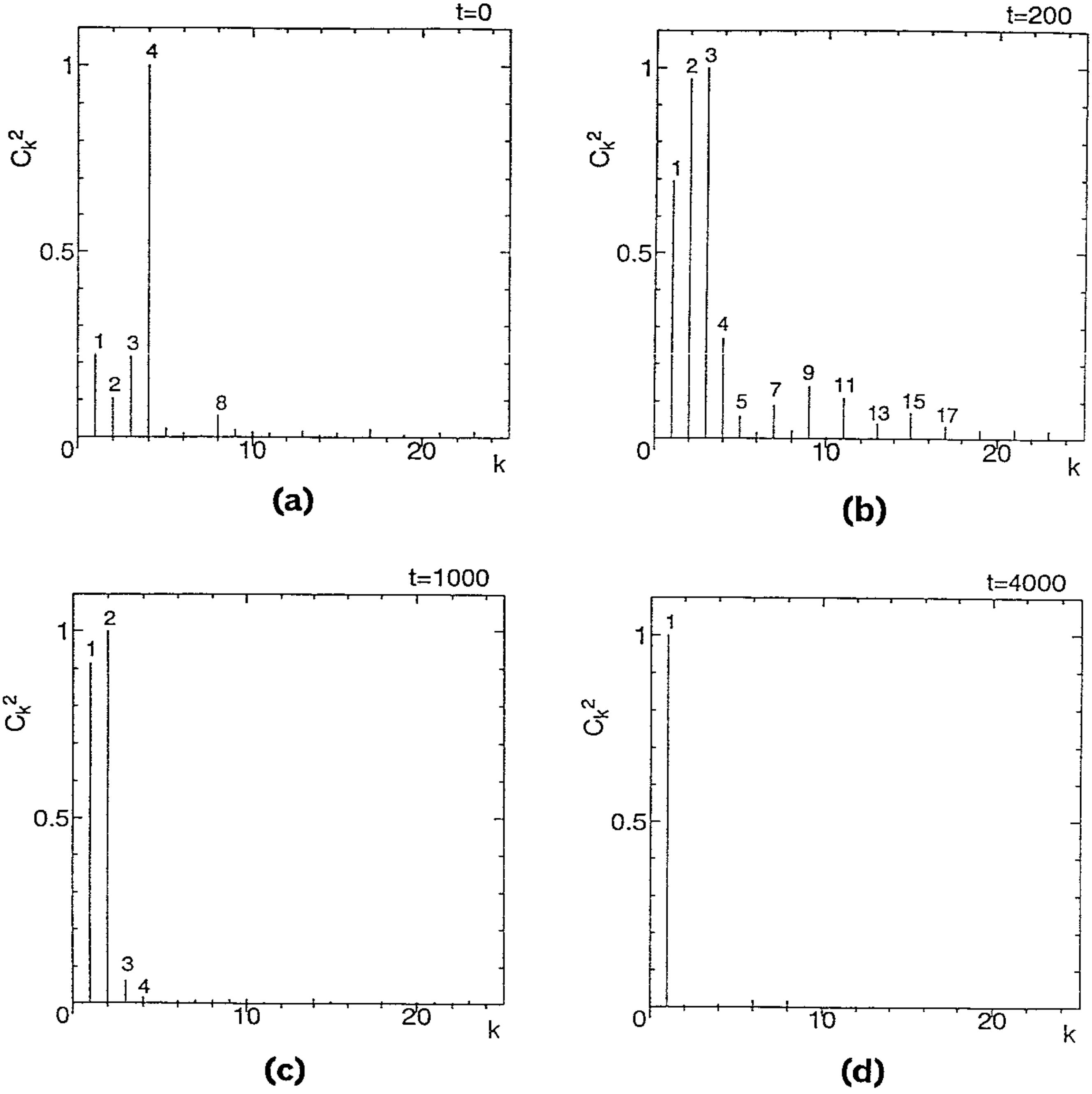

Fig. 2

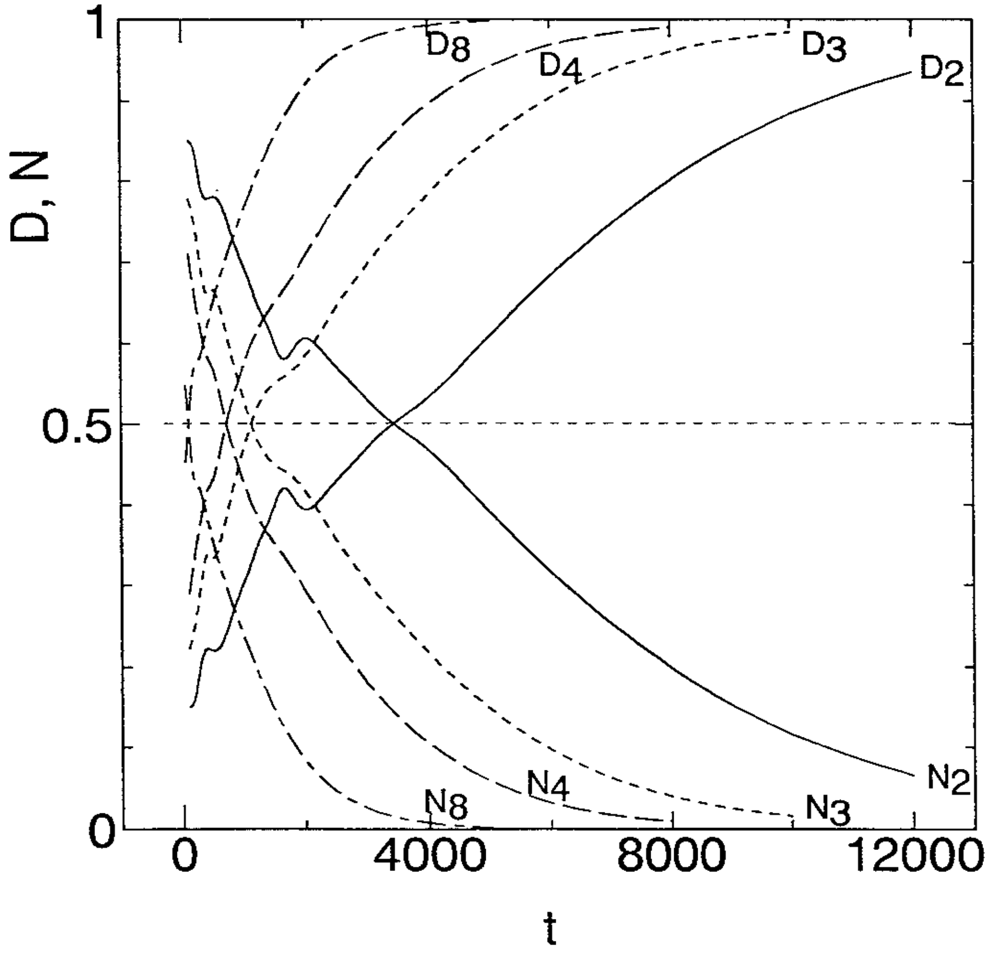

Fig. 3

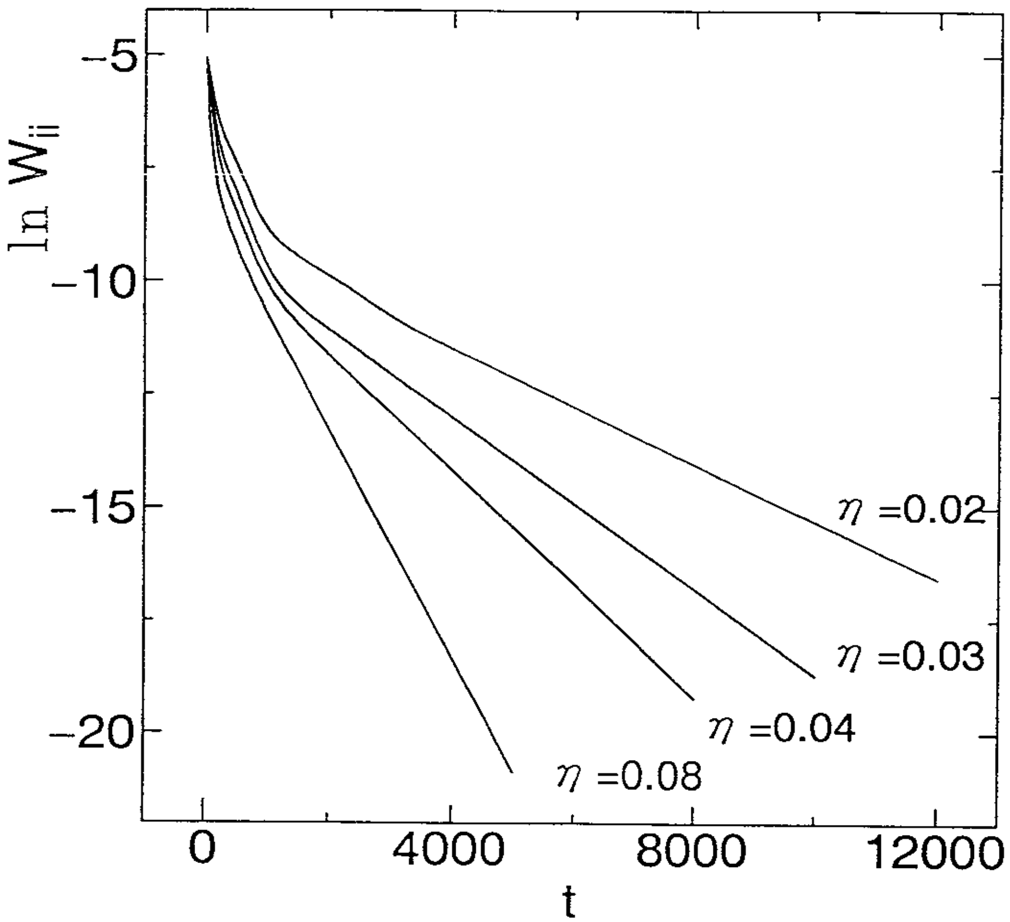

Fig. 4

Recent Issues of NIFS Series

NIFS-332 N. Bekki and T. Karakisawa,
Bifurcations from Periodic Solution in a Simplified Model of Two-dimensional Magnetoconvection; Jan. 1995

NIFS-333 K. Itoh, S.-I. Itoh, M. Yagi, A. Fukuyama,
Theory of Anomalous Transport in Reverse Field Pinch; Jan. 1995

NIFS-334 K. Nagasaki, A. Isayama and A. Ejiri
Application of Grating Polarizer to 106.4GHz ECH System on Heliotron-E; Jan. 1995

NIFS-335 H. Takamaru, T. Sato, R. Horiuchi, K. Watanabe and Complexity Simulation Group,
A Self-Consistent Open Boundary Model for Particle Simulation in Plasmas; Feb. 1995

NIFS-336 B.B. Kadomtsev,
Quantum Telegragh : is it possible?; Feb. 1995

NIFS-337 B.B.Kadomtsev,
Ball Lightning as Self-Organization Phenomenon; Feb. 1995

NIFS-338 Y. Takeiri, A. Ando, O. Kaneko, Y. Oka, K. Tsumori, R. Akiyama, E. Asano, T. Kawamoto, M. Tanaka and T. Kuroda,
High-Energy Acceleration of an Intense Negative Ion Beam; Feb. 1995

NIFS-339 K. Toi, T. Morisaki, S. Sakakibara, S. Ohdachi, T.Minami, S. Morita, H. Yamada, K. Tanaka, K. Ida, S. Okamura, A. Ejiri, H. Iguchi, K. Nishimura, K. Matsuoka, A. Ando, J. Xu, I. Yamada, K. Narihara, R. Akiyama, H. Idei, S. Kubo, T. Ozaki, C. Takahashi, K. Tsumori,
H-Mode Study in CHS; Feb. 1995

NIFS-340 T. Okada and H. Tazawa,
Filamentation Instability in a Light Ion Beam-plasma System with External Magnetic Field; Feb. 1995

NIFS-341 T. Watanbe, G. Gnudi,
A New Algorithm for Differential-Algebraic Equations Based on HIDM; Feb. 13, 1995

NIFS-342 Y. Nejoh,
New Stationary Solutions of the Nonlinear Drift Wave Equation; Feb. 1995

NIFS-343 A. Ejiri, S. Sakakibara and K. Kawahata,
Signal Based Mixing Analysis for the Magnetohydrodynamic Mode

Reconstruction from Homodyne Microwave Reflectometry; Mar.. 1995

NIFS-344 B.B.Kadomtsev, K. Itoh, S.-I. Itoh
Fast Change in Core Transport after L-H Transition; Mar. 1995

NIFS-345 W.X. Wang, M. Okamoto, N. Nakajima and S. Murakami,
An Accurate Nonlinear Monte Carlo Collision Operator; Mar. 1995

NIFS-346 S. Sasaki, S. Takamura, S. Masuzaki, S. Watanabe, T. Kato, K. Kadota,
Helium I Line Intensity Ratios in a Plasma for the Diagnostics of Fusion Edge Plasmas; Mar. 1995

NIFS-347 M. Osakabe,
Measurement of Neutron Energy on D-T Fusion Plasma Experiments; Apr. 1995

NIFS-348 M. Sita Janaki, M.R. Gupta and Brahmananda Dasgupta,
Adiabatic Electron Acceleration in a Cnoidal Wave; Apr. 1995

NIFS-349 J. Xu, K. Ida and J. Fujita,
A Note for Pitch Angle Measurement of Magnetic Field in a Toroidal Plasma Using Motional Stark Effect; Apr. 1995

NIFS-350 J. Uramoto,
Characteristics for Metal Plate Penetration of a Low Energy Negative Muonlike or Pionlike Particle Beam: Apr. 1995

NIFS-351 J. Uramoto,
An Estimation of Life Time for A Low Energy Negative Pionlike Particle Beam: Apr. 1995

NIFS-352 A. Taniike,
Energy Loss Mechanism of a Gold Ion Beam on a Tandem Acceleration System: May 1995

NIFS-353 A. Nishizawa, Y. Hamada, Y. Kawasumi and H. Iguchi,
Increase of Lifetime of Thallium Zeolite Ion Source for Single-Ended Accelerator: May 1995

NIFS-354 S. Murakami, N. Nakajima, S. Okamura and M. Okamoto,
Orbital Aspects of Reachable β Value in NBI Heated Heliotron/Torsatrons; May 1995

NIFS-355 H. Sugama and W. Horton,
Neoclassical and Anomalous Transport in Axisymmetric Toroidal Plasmas with Electrostatic Turbulence; May 1995

NIFS-356 N. Ohyabu
A New Boundary Control Scheme for Simultaneous Achievement

of H-mode and Radiative Cooling (SHC Boundary); May 1995

NIFS-357 Y. Hamada, K.N. Sato, H. Sakakita, A. Nishizawa, Y. Kawasumi, R. Liang, K. Kawahata, A. Ejiri, K. Toi, K. Narihara, K. Sato, T. Seki, H. Iguchi, A. Fujisawa, K. Adachi, S. Hidekuma, S. Hirokura, K. Ida, M. Kojima, J. Koong, R. Kumazawa, H. Kuramoto, T. Minami,. M. Sasao, T. Tsuzuki, J.Xu, I. Yamada, and T. Watari,
Large Potential Change Induced by Pellet Injection in JIPP T-IIU Tokamak Plasmas; May 1995

NIFS-358 M. Ida and T. Yabe,
Implicit CIP (Cubic-Interpolated Propagation) Method in One Dimension; May 1995

NIFS-359 A. Kageyama, T. Sato and The Complexity Simulation Group,
Computer Has Solved A Historical Puzzle: Generation of Earth's Dipole Field; June 1995

NIFS-360 K. Itoh, S.-I. Itoh, M. Yagi and A. Fukuyama,
Dynamic Structure in Self-Sustained Turbulence; June 1995

NIFS-361 K. Kamada, H. Kinoshita and H. Takahashi,
Anomalous Heat Evolution of Deuteron Implanted Al on Electron Bombardment; June 1995

NIFS-362 V.D. Pustovitov,
Suppression of Pfirsch-schlüter Current by Vertical Magnetic Field in Stellarators; June 1995

NIFS-363 A. Ida, H. Sanuki and J. Todoroki
An Extended K-dV Equation for Nonlinear Magnetosonic Wave in a Multi-Ion Plasma; June 1995

NIFS-364 H. Sugama and W. Horton
Entropy Production and Onsager Symmetry in Neoclassical Transport Processes of Toroidal Plasmas; July 1995

NIFS-365 K. Itoh, S.-I. Itoh, A. Fukuyama and M. Yagi,
On the Minimum Circulating Power of Steady State Tokamaks; July 1995

NIFS-366 K. Itoh and Sanae-I. Itoh,
The Role of Electric Field in Confinement; July 1995

NIFS-367 F. Xiao and T. Yabe,
A Rational Function Based Scheme for Solving Advection Equation; July 1995

NIFS-368 Y. Takeiri, O. Kaneko, Y. Oka, K. Tsumori, E. Asano, R. Akiyama,

T. Kawamoto and T. Kuroda,
Multi-Beamlet Focusing of Intense Negative Ion Beams by Aperture Displacement Technique; Aug. 1995

NIFS-369 A. Ando, Y. Takeiri, O. Kaneko, Y. Oka, K. Tsumori, E. Asano, T. Kawamoto, R. Akiyama and T. Kuroda,
Experiments of an Intense H- Ion Beam Acceleration; Aug. 1995

NIFS-370 M. Sasao, A. Taniike, I. Nomura, M. Wada, H. Yamaoka and M. Sato,
Development of Diagnostic Beams for Alpha Particle Measurement on ITER; Aug. 1995

NIFS-371 S. Yamaguchi, J. Yamamoto and O. Motojima;
A New Cable -in conduit Conductor Magnet with Insulated Strands; Sep. 1995

NIFS-372 H. Miura,
Enstrophy Generation in a Shock-Dominated Turbulence; Sep. 1995

NIFS-373 M. Natsir, A. Sagara, K. Tsuzuki, B. Tsuchiya, Y. Hasegawa, O. Motojima,
Control of Discharge Conditions to Reduce Hydrogen Content in Low Z Films Produced with DC Glow; Sep. 1995

NIFS-374 K. Tsuzuki, M. Natsir, N. Inoue, A. Sagara, N. Noda, O. Motojima, T. Mochizuki, I. Fujita, T. Hino and T. Yamashina,
Behavior of Hydrogen Atoms in Boron Films during H_2 and He Glow Discharge and Thermal Desorption; Sep. 1995

NIFS-375 U. Stroth, M. Murakami, R.A. Dory, H. Yamada, S. Okamura, F. Sano and T. Obiki,
Energy Confinement Scaling from the International Stellarator Database; Sep. 1995

NIFS-376 S. Bazdenkov, T. Sato, K. Watanabe and The Complexity Simulation Group,
Multi-Scale Semi-Ideal Magnetohydrodynamics of a Tokamak Plasma; Sep. 1995

NIFS-377 J. Uramoto,
Extraction of Negative Pionlike Particles from a H2 or D2 Gas Discharge Plasma in Magnetic Field; Sep. 1995

NIFS-378 K. Akaishi,
Theoretical Consideration for the Outgassing Characteristics of an Unbaked Vacuum System; Oct. 1995

NIFS-379 H. Shimazu, S. Machida and M. Tanaka,
Macro-Particle Simulation of Collisionless Parallel Shocks; Oct. 1995